

Conductance of open quantum billiards and classical trajectoriesR. G. Nazmitdinov,^{1,2,*} K. N. Pichugin,^{3,4,†} I. Rotter,^{1,‡} and P. Šeba^{3,5,§}¹Max-Planck-Institut für Physik komplexer Systeme, D-01187 Dresden, Germany²Joint Institute for Nuclear Research, 141980 Dubna, Russia³Institute of Physics, Czech Academy of Sciences, 16253 Prague, Czech Republic⁴Kirensky Institute of Physics, 660036 Krasnoyarsk, Russia⁵Department of Physics, University Hradec Kralove, 50003 Hradec Kralove, Czech Republic

(Received 16 November 2001; revised manuscript received 20 February 2002; published 23 August 2002)

We analyze the transport phenomena of two-dimensional quantum billiards with convex boundary of different shape. The quantum mechanical analysis is performed by means of the poles of the S matrix while the classical analysis is based on the motion of a free particle inside the cavity along trajectories with a different number of bounces at the boundary. The value of the conductance depends on the manner in which the leads are attached to the cavity. The Fourier transform of the transmission amplitudes is compared with the length of the classical paths. There is good agreement between classical and quantum mechanical results when the conductance is achieved mainly by special short-lived states such as whispering gallery modes and bouncing ball modes. In these cases, also the localization of the wave functions agrees with the picture of the classical paths. The S matrix is calculated classically and compared with the transmission coefficients of the quantum mechanical calculations for five modes in each lead. The number of modes coupled to the special states is effectively reduced.

DOI: 10.1103/PhysRevB.66.085322

PACS number(s): 73.23.Ad, 05.60.-k, 03.65.-w

I. INTRODUCTION

The problem of whether and how classical dynamics of mesoscopic systems is manifest in quantum mechanical characteristics is studied intensively during the past decade. It is well established that the statistical fluctuations of quantum systems whose associated classical dynamics is chaotic are well described by random matrix theory, see Ref. 1 and the recent reviews.²⁻⁴ This approach treats the spectra of many dense lying states by means of statistical methods neglecting the individual properties of the states.⁵ In other studies, the relation between the quantum conductance fluctuations and the classical chaotic dynamics has been established on the basis of the semiclassical approach to the S matrix.^{6,7}

In quantum systems with low-level density, *deviations from the randomness* are observed and discussed, both theoretically and experimentally.⁸⁻²⁰ The results point at quantum mechanical interference effects between the quantum states, which may become important under certain conditions. These effects are displayed, e.g., in the transport phenomena through quantum dots, when the leads are configured in such a manner that one or a few propagating modes are supported.¹⁴⁻¹⁶ The underlying processes are not fully understood, up to now. A detailed analysis of the internal structure of the corresponding Hamiltonian is therefore required. Here, new questions arise such as (i) which role do the individual properties of the states play whose small number in a certain energy region does, generally, not allow a statistical description, (ii) which states survive when the system is embedded into an environment, and (iii) what is the relation between classical and quantum mechanical characteristics under these conditions.

A study of these problems in real systems is difficult since their separation from other questions such as many-body correlations and the shape of the effective potential is impos-

sible. The most transparent answers are expected from a study of microwave cavities which simulate well the features of real quantum systems.²¹ In this case, the shape of the system is well defined and two-body forces do not exist.

Generic features of regular and chaotic dynamics in quantum transport have been found in open quantum billiards of different shape at energies where *many* channels are open. If the scattering dynamics is classically chaotic, conductance fluctuations exhibit an universal behavior^{6,7} describable by the random matrix theory, see the reviews.²⁻⁴ The fluctuations are related to long classical trajectories. The analysis of the conductance fluctuations of a stadium *weakly* coupled to a *small* number of channels shows, however, that the conductance fluctuations carry clear signatures of classical trajectories with short path lengths.⁹ These trajectories have been associated with those of whispering gallery type. A similar conclusion has been drawn on the basis of the generalized semiclassical scattering approach applied to the analysis of transport through a circular billiard.¹⁰ In this case, asterisk trajectories dominate in the power spectrum, while the whispering gallery ones are not important. That means, the short trajectories contribute essentially to the conductance fluctuations at low energy. It should be mentioned, however, that the relation of these trajectories to the eigenstates and eigenfunctions of the corresponding quantum Hamiltonian of the closed system has not been discussed in these papers.

Theoretical and experimental studies on microwave cavities and also on quantum dots which are coupled *strongly* to a *small* number of channels, have shown that the individual properties of the states and their matching to the wave functions of the environment play an important role under these conditions.^{14,15,22-25} Analytical considerations show that a level repulsion as well as a level clustering may appear. The repulsion of the states in energy is accompanied by adjusting

their widths (inverse lifetimes of the states) while the clustering of levels is accompanied by a bifurcation of the widths. Both phenomena are observed, in fact, in numerical studies on rectangular billiards in which the matching of the wave functions is varied by means of enlarging (or reducing) the area of the cavity.²³ Clusters in the tunneling resonance spectra of ultrasmall metallic particles of the size of a few nanometers have been observed experimentally¹² and explained theoretically.¹³

The wave-function statistics for ballistic quantum transport through chaotic open billiards is investigated in Ref. 20. Here, the chaotic-scattering wave functions in open systems are interpreted quantitatively in terms of statistically independent real *and* imaginary random fields in the same manner as for wave-function statistics of closed systems. This result may be compared with a similar one obtained from an analysis of the nuclear coupling to the one-channel continuum.²⁶ The Gaussian distribution of both, the real and imaginary parts, seems therefore to be a common feature of the wave-function statistics of small open quantum systems.

The role of the matching of the wave functions for the dynamics of the system is studied further in Ref. 24. Here, some special states are shown to accumulate the total coupling strength between system and environment, which is expressed by the sum of the widths of all states lying in the energy region considered. The accumulation takes place by resonance trapping, i.e., all states but the special ones decouple more or less from the environment while the widths of the special states reach the maximum possible value.

The quantum billiard considered in Ref. 24 has the shape of a semicircle with an internal scatterer (SIS). It is coupled strongly to the attached leads. Here, bands of overlapping resonance states appear whose wave functions are localized either along the convex boundary of the cavity or along the direct connection between the two attached leads. The first type of resonances is related to whispering gallery modes (WGM) and the other one to bouncing ball modes (BBM). The transition from one type to the other is traced in Ref. 24 by varying the position of one of the two attached leads. As a result, the BBM being special states at a certain position of the attached leads, are trapped by the WGM at another position of the leads. The internal scatterer in the SIS does not play any role in this phenomenon since it appears in a quantum billiard of semicircle shape without any internal scatterer as well. Meanwhile, the phenomenon of resonance trapping has been proven experimentally.²⁷

The whispering gallery modes exist in closed systems with a convex boundary (see Ref. 19 and references therein). As is mentioned above, they are observed also for weakly opened quantum billiards.⁹ The conclusion can therefore be drawn that they are special states of the system which survive at strong coupling to the environment and give, under certain conditions, a large contribution to observable values, e.g., to the transmission (conductance). Besides these special states there exist, at the same energy, a large number of long-lived states that are decoupled more or less from the environment and contribute incoherently to the observables. The transmission shows a gross structure caused by the special states and a fine structure (fluctuations) created by the inter-

ferences with the long-lived trapped states. Accordingly, a Fourier analysis of the transmission spectrum contains information not only on the long-lived states but also on the special states.

In the present paper, we consider quantum billiards of Bunimovich type with different positions of the attached leads under the condition of *strong coupling* between billiard and leads. Since the closed Bunimovich billiard shows the features of chaotic dynamics, this system is especially suited for the study of the question of which states survive after embedding it into an environment. We will show that an appropriate attachment of the leads selects special states, which enhances the conductance as compared to the predictions of random matrix theory. Further, we compare the results of a Fourier analysis of the transmission spectra with the results of classical calculations for the conductance of cavities having the same geometry. This comparison will provide us information on the question of the degree to which classical properties of dynamical systems are manifest in quantum mechanical characteristics, in particular in the phenomenon of transport through strongly opened billiards with both a small number of states and a small number of open channels.

The paper is organized as follows. In Sec. II, the basic equations underlying the quantum mechanical description are given. In Sec. III, we provide the results obtained numerically for quantum billiards of Bunimovich type to which the leads are coupled in a different manner. They are configured to support a small number of propagating modes (≤ 5). We represent the eigenvalue pictures together with some wave functions and the power spectra obtained from the Fourier analysis of the transmission and reflection fluctuations. The values are compared with those calculated classically. Furthermore, the S matrix is calculated classically and compared with the transmission coefficients of the quantum mechanical calculation for five modes in each channel. The results are discussed in Sec. IV and summarized in the last section.

II. BASIC EQUATIONS OF THE QUANTUM MECHANICAL DESCRIPTION

We consider a two-dimensional (2D) flat resonator coupled to two leads and solve the 2D Schrödinger equation

$$-\frac{\hbar^2}{2m}\Delta\Psi = E\Psi \quad (1)$$

under the assumption that the potential is zero inside the billiard and inside the leads but infinite outside these regions. The walls are assumed to be infinitely hard. In other words, we use the Dirichlet boundary condition $\Psi = 0$ on the boundary of the billiard and of the leads. The wave functions inside the leads are given as a superposition of plane waves,

$$\Psi_1(x,y) = \sum_{m=1}^Z (a_m e^{ik_m x} + b_m e^{-ik_m x}) u_m(y),$$

$$\Psi_2(x,y) = \sum_{n=1}^Z (a_n e^{ik_n x} + b_n e^{-ik_n x}) u_n(y), \quad (2)$$

where we denote the two leads by 1 and 2, respectively, $u_j(y) = \sqrt{[2/(dk_n)]} \sin([\pi j/d]y)$, $j = n, m$. Further, d is the width of each lead and $m(n) = 1, 2, \dots, Z$ is the number of transversal modes in lead 1(2). The wave number is $k_n = \sqrt{2m_{\text{eff}}/\hbar^2 (E - E_n)}$ where $E_n = \hbar^2 n^2 \pi^2 / (2m_{\text{eff}} d^2)$ is the energy associated with the transverse motion. At the energy E the modes n with $E - E_n > 0$ are propagating while those with $E < E_n$ are evanescent waves. In the following, we use the units $\hbar^2/(2m_{\text{eff}}) = 1$ and choose $d = 1$.

By definition, the S matrix maps the amplitudes of incoming waves to those of the outgoing ones,

$$b = Sa. \quad (3)$$

The S matrix can be written as

$$S_{cc'} = S_{cc'}^{(1)} - S_{cc'}^{(2)}, \quad (4)$$

where $S_{cc'}^{(1)}$ contains the smooth direct reaction part and

$$S_{cc'}^{(2)} = 2i\pi \sum_{R=1}^N \frac{\tilde{W}_R^{c'} \tilde{W}_R^c}{E - \tilde{E}_R + \frac{i}{2}\tilde{\Gamma}_R} \quad (5)$$

is the resonance reaction part in pole representation (for details, see Refs. 8 and 28). Here, the c denote the channels $m = 1, \dots, Z$, $n = 1, \dots, Z$. The $\tilde{E}_R - (i/2)\tilde{\Gamma}_R$ are the complex eigenvalues of the non-Hermitian effective Hamiltonian H_{eff} . The eigenfunctions $\tilde{\Phi}_R$ of H_{eff} are biorthogonal. Both, the eigenvalues and eigenfunctions are energy dependent. The eigenvalues give the energies $E_R = \tilde{E}_R (E = E_R)$ and widths $\Gamma_R = \tilde{\Gamma}_R (E = E_R)$ of the *resonance* states of the billiard by solving the fixed-point equations. The E_R and Γ_R are directly related to the poles of the S matrix. The \tilde{W}_R^c are the (complex) coupling matrix elements between the wave functions $\tilde{\Phi}_R$ of the *resonance* states and the channel wave functions in the leads [by using the Lippmann-Schwinger-type relation between the wave functions $\tilde{\Omega}_R$ of the resonance states and the eigenfunctions $\tilde{\Phi}_R$ of the non-Hermitian effective Hamiltonian H_{eff} (Refs. 8, 28 and 29)]. They are strongly energy dependent, but $\Gamma_R = 2\pi \sum_c (W_R^c)^2$ at $E = E_R$ due to the unitarity of the S matrix [with $(W_R^c)^2 = (\tilde{W}_R^c)^2 (E = E_R)$]. The expression (5) holds also in the strong coupling limit, i.e., not only for isolated resonance states but also for overlapping ones.^{8,28} Formally, this is related to the fact that all values involved in Eq. (5) are characteristic of the *resonance* states that generically differ from the discrete states in the case of strong coupling between system and environment.

A similar approach has been developed in Ref. 30, but without application to realistic systems. In Ref. 3, the expression for the S matrix is given in terms of a Green function with a non-Hermitian effective Hamiltonian, and the complex poles are identified as eigenvalues of this operator. The

approximate expressions, obtained in this approach, can be applied in the limit of weak coupling.

Although the expression $S_{cc'}^{(2)}$, Eq. (5), formally has the standard form, it contains all the reordering processes taking place in the system at strong coupling, i.e., when the resonance states overlap, including the influence of the channel-channel coupling. All these effects are expressed by the biorthogonality of the wave functions $\tilde{\Phi}_R$ and are involved in the energy-dependent functions \tilde{W}_R^c , \tilde{E}_R , and $\tilde{\Gamma}_R$. The representation of the S matrix as a sum of the contributions from the individual resonance states with energy-independent E_R , Γ_R , and W_R^c is, generally, not justified. We calculate the S matrix therefore by employing the full energy dependence of the \tilde{W}_R^c , \tilde{E}_R , and $\tilde{\Gamma}_R$. At the fixed points $E = E_R$, the results coincide with those obtained from the corresponding pole term.

For *isolated* resonances the widths of the states are much smaller than the distance between them. In such a case, $\tilde{E}_R \approx E_R^d$, $\tilde{W}_R^c \approx W_R^{c(d)}$, and the channels are not coupled. That means, the S matrix poles can be calculated with the help of the coupling matrix elements $W_R^{c(d)}$ (overlap integrals between the wave functions Φ_R^d of the discrete states and the channel wave functions u_n in the leads), with the energies E_R^d of the discrete states of the (closed) billiard and $\Gamma_R^d = 2\pi \sum_c (W_R^{c(d)})^2$. This approximation is justified for the description of S matrix poles lying near the real axis.³¹

For *overlapping* resonances (i.e. when the widths exceed the energetical distance between the resonances), the \tilde{E}_R and \tilde{W}_R^c may differ strongly from the E_R^d and $W_R^{c(d)}$, respectively, due to reordering processes taking place in the billiard under the influence of the coupling to the leads. For numerical examples see Refs. 22–24. Due to these reordering processes, the S matrix cannot be approximated by using the energy-independent E_R and W_R^c as shown in a numerical study.³² Instead, the \tilde{E}_R , $\tilde{\Gamma}_R$ and, above all, the \tilde{W}_R^c in (5) are energy-dependent functions that characterize the *resonance* states and their coupling to the continuum. Moreover, in Ref. 33 the effective Hamiltonian for an open quantum billiard with variable coupling strength to an attached lead is derived. Diagonalizing this effective Hamiltonian, numerical studies are performed for billiards with isolated and overlapping resonances. The results are in good agreement with experimental data obtained from microwave resonators of the same shape.³³ In particular, the phenomenon of resonance trapping can clearly be seen in both the theoretical and experimental results. These results confirm that Eq. (5) can be used in the strong coupling regime.

Reordering processes may take place in open quantum systems *not only* between the states of the system which cause the wave functions $\tilde{\Phi}_R$ of the resonance states to be different from the wave functions Φ_R^d of the discrete states. The strong coupling of some resonance states to the channel wave functions may cause also changes in the channel wave functions themselves because they are coupled via the resonance states. This coupling of the channel wave functions via the resonance states (channel-channel coupling) is in com-

plete resemblance to the coupling of the resonance states via the channels. Both are caused by the same coupling matrix elements between the resonance wave functions and the channel wave functions. For details see Ref. 8. Wave functions of different channels may couple so strongly as to effectively appear as a one-channel wave function and exist together with less coupled channel wave functions. Thus, the number of relevant channels may be effectively reduced at strong coupling between system and environment. For numerical examples on quantum billiards, see Ref. 24 and for nuclei see Ref. 26.

Since the sum of the diagonal matrix elements of a matrix is equal to the sum of the eigenvalues, we get^{8,28}

$$\sum_R \tilde{\Gamma}_R = 2\pi \sum_{Rc} (\tilde{W}_R^c)^2 = 2\pi \sum_{Rc} (W_R^{c(d)})^2 = \sum_R \Gamma_R^d, \quad (6)$$

where the Γ_R^d characterize the coupling of the states R to the environment without taking into account any mixing (via the continuum) with the other states of the system. Equation (6) gives the total coupling strength between system and environment. It is basic for all redistribution processes taking place in the system under the influence of the coupling to the environment. This is confirmed in particular for redistributions that happen in the quantum billiard when the position of the attached leads to the billiard is varied.²⁴ In this case,

$$\sum_R \tilde{\Gamma}_R = 2\pi \sum_{Rc} (\tilde{W}_R^c)^2 \approx \text{const} \quad (7)$$

since the $W_R^{c(d)}$ are determined by an integral over the region of attachment^{32,33} and remain almost unchanged by varying the position of the attachment (if the number of states in the cavity is not too small). It may happen that, under certain conditions,

$$\sum_{R=1}^K \tilde{\Gamma}_R \approx \sum_{R=1}^M \tilde{\Gamma}_R \quad \text{and} \quad \sum_{R=K+1}^M \tilde{\Gamma}_R \approx 0. \quad (8)$$

In such a case, the whole coupling strength is concentrated on $K < M$ special states while $M - K$ states are almost decoupled from the environment. This phenomenon, called *resonance trapping*,⁸ is crucial for the conductance of quantum billiards with WGM.²⁴ The value of K may or may not be related to the number Z of open channels.⁸ For the WGM, K is determined, in a certain energy interval, by the number of nodes along the (convex) boundary of the cavity leading to $K \gg 1$ in the one-channel case.²⁴

For the analysis of transmission and reflection of quantum billiards with two leads attached to them, it is convenient to write the S matrix in the following manner:²

$$\begin{pmatrix} S_{mm'} & S_{mn} \\ S_{nm} & S_{nn'} \end{pmatrix} \equiv \begin{pmatrix} r & t' \\ t & r' \end{pmatrix}. \quad (9)$$

Here, $m(n)$ denote the channels in lead 1(2). The matrices r and r' describe the reflection in the lead 1 and 2, respectively, while the matrices t and t' describe the transmission from lead 1 to lead 2 and vice versa. The total transmission and reflection probabilities for the modes m are

$$T_m = \sum_{n=1}^Z |t_{mn}|^2 \quad \text{and} \quad R_m = \sum_{m'=1}^Z |r_{mm'}|^2, \quad (10)$$

respectively. As shown by Landauer,^{2,4} the conductance G is proportional to the sum of the transmission probabilities,

$$G = \sum_m T_m \quad (11)$$

in the units used by us (see above). The fluctuations in the transmission and reflection amplitudes can be analyzed by means of a Fourier transformation,

$$|t_{mn}(L)|^2 = \left| \int dk t_{mn}(k) e^{-ikL} \right|^2 = \left| \int \frac{dE}{2\sqrt{E}} t_{mn}(E) e^{-i\sqrt{E}L} \right|^2. \quad (12)$$

The sum

$$P(L) = \sum_{mn} |t_{mn}(L)|^2 \quad (13)$$

is called the power spectrum.³⁴ An analogous expression can be written down for the Fourier transform of the reflection amplitudes.

It should be noted that the power spectrum (13) can be related to the autocorrelation function of the conductance. To this purpose, we use the Fourier transform

$$P(L) = \int dk C(k) e^{-ikL}, \quad (14)$$

where

$$C(k) = \left\langle t_{mn}^* \left(k' - \frac{k}{2} \right) t_{mn} \left(k' + \frac{k}{2} \right) \right\rangle_{k'} \quad (15)$$

is the autocorrelation function of the conductance averaged over k' (or energy) which is studied in Refs. 6 and 7. According to the semiclassical formalism of the ballistic transport^{6,7,10} the transmission amplitude t_{mn} is

$$t_{mn}(k) = \sum_q a_q e^{ikL_q}, \quad (16)$$

where the sum is taken over the path q with a length L_q between the entrance and exit leads. The detailed structure of the coefficient a_q can be found in Refs. 7 and 10.

III. NUMERICAL RESULTS

A. Quantum mechanical and classical calculations

We study a stadium of Bunimovich type [linear length $S = 3\pi/(\pi+1)$ and radius $R=S$] in the ballistic regime with different positions of the attached leads. The results are compared with those of a semicircle ($R=3$) with an SIS and leads attached to both ends of the convex boundary.

In the first case ($B1$) of the Bunimovich billiard, the leads are attached to the middle of each convex boundary in the same direction so that the WGM are favored for the conductance, i.e., the coupling matrix elements $W_R^{c(d)}$ of the WGM

with the channel waves are large. This case is in full analogy to the SIS. In the second case (*B2*), the leads are attached to the middle of each linear boundary in opposite directions so that the BBM are favored for the conductance. In the third case (*B3*), the leads are attached to the convex boundary in different directions in such a manner that neither WGM nor BBM are favored for the conductance. We compared the results with those of classical calculations for billiards with the same geometry.

To find the poles of the S matrix, we use the method of the exterior complex scaling in combination with the finite-element method. For details see Ref. 22. The results of the calculations give us the values $E_R - (i/2)\Gamma_R = \tilde{E}_R(E = E_R) - (i/2)\tilde{\Gamma}_R(E = E_R)$ (in fact, approximate solutions of the fixed-point equations, see Sec. II). The conductance is calculated in small energy steps with the full energy dependence of the S matrix by directly solving the Schrödinger equation in a discretized space according to the method suggested in Ref. 35. The essential ingredients are the conductance formulas (10) and (11), the relation of transmission coefficients to the S matrix and the corresponding Green function, and a recursive calculation of the Green function. At the fixed points $E = E_R$, the results coincide with those obtained from the complex scaling. At other energies, the interfering contributions of different resonance states can be obtained more effectively without searching for the poles of the S matrix.

The Fourier analysis of the transmission and reflection amplitudes provides us the power spectrum $P(L)$ for one open channel (one propagating mode, $m = n = 1$) and for two open channels ($m = 1, 2, n = 1, 2$) in both leads according to Eqs. (12) and (13).

In the classical calculations, we consider the motion of a free particle inside the billiard. The potential is assumed to be zero inside the billiard and the boundaries are mirrors for the motion of the particle along trajectories that are calculated from the laws of the geometric optics. Each trajectory starts at some arbitrarily chosen initial point (x_0, y_0) of the attached leads with an angle Φ_0 that characterizes the direction of the motion. We choose 1000×1000 initial conditions to calculate the distribution (histogram) of the trajectories that contribute to the transport. The classical conductance is defined as the number of trajectories starting at one of the leads and escaping from the other one, divided by the total number of trajectories (10^6). Trajectories with bounces at the convex boundary only are called *trajectories of WGM type* in the following. The number of such trajectories decreases with increasing number of bounces, see, e.g., Fig. 3 in Ref. 24.

B. Eigenvalue pictures

Figure 1 shows the results of numerical calculations for the four quantum billiards mentioned above. For the SIS we find, as in Ref. 24, bands *A*, *B*, and *C* of overlapping resonance states whose widths are large, while the widths of all the other states are small [Fig. 1(a)]. The short-lived states of the bands *A*, *B*, and *C* start at the opening of thresholds at $E = \pi^2, 4\pi^2, 9\pi^2$, respectively. At energies $E > 4\pi^2$, we have channel wave functions that are effectively coupled to

the one-channel mode. They exist besides the less coupled channel wave functions.²⁴ In an analogous manner, the channel wave functions may be effectively coupled to one or two modes beyond $E = 9\pi^2$.

The eigenvalue picture Fig. 1(a) is the result of resonance trapping occurring according to Eq. (8) and of channel-channel coupling, see Sec. II. The states with large widths are localized along the convex boundary of the cavity [Fig. 1(b) and Ref. 24]. They are modes of the WGM type. The states of the band *A* have a strong overlap with effectively one open channel in both leads at all energies. The states of the second band *B* are related to effectively two open channels in each lead while the states of the band *C* are related to three channels. At higher energies, the states of the different bands interact with one another, and the structure of the resonance wave functions represents a mixture of the states of different bands.

The results for the billiard *B1* [Figs. 1(c,d)] are very similar to those for the SIS. The difference in the widths of the short-lived and long-lived states is, however, smaller and the wave functions of the *B1* are less localized than those of the SIS. This is caused by modes of the WGM type localized along the lower boundary of the *B1*. Such modes are coupled weakly to the attached leads.

The attaching of the leads at the linear boundary [*B2*; Figs. 1(e,f)] gives rise to large widths for states of the BBM type. The differences between the WGM and BBM consist in the following.

The WGM are localized along the boundary of the cavity while the BBM are localized inside the billiard along the direct connection between the two attached leads.

The number of the BBM as well as the degree of their overlapping in the complex plane are smaller than the corresponding values for the WGM in the same cavity.

The BBM do trap the other states less than the WGM do, i.e., some other states (in particular those of the WGM type) still survive in the *B2* with small but nonzero widths. These states take, for example, altogether about 17% of the total sum $\sum_R \tilde{\Gamma}_R$ of the widths for $\pi^2 < E < 4\pi^2$.

In the *B3* billiard [Figs. 1(g,h)] the coupling matrix elements of the WGM are large but with different phase in relation to the two leads. As in the two foregoing cases, the poles with the largest widths are connected with one another for illustration. The wave function of one of the states is shown in Fig. 1(h) which is, however, less representative for a certain group of states than in the foregoing cases [Figs. 1(b,d,f)].

C. Power spectra and classical trajectories

In Fig. 2, we present the (energy-dependent) conductance G calculated quantum mechanically and the mean value \bar{G} of the conductance. Furthermore, we show in this figure, the corresponding power spectra $P(L)$ and the histograms of trajectories calculated classically for transmission as a function of the length L of the path for the four different types of billiards. The results display a remarkable good agreement between the quantum mechanical results of the Fourier

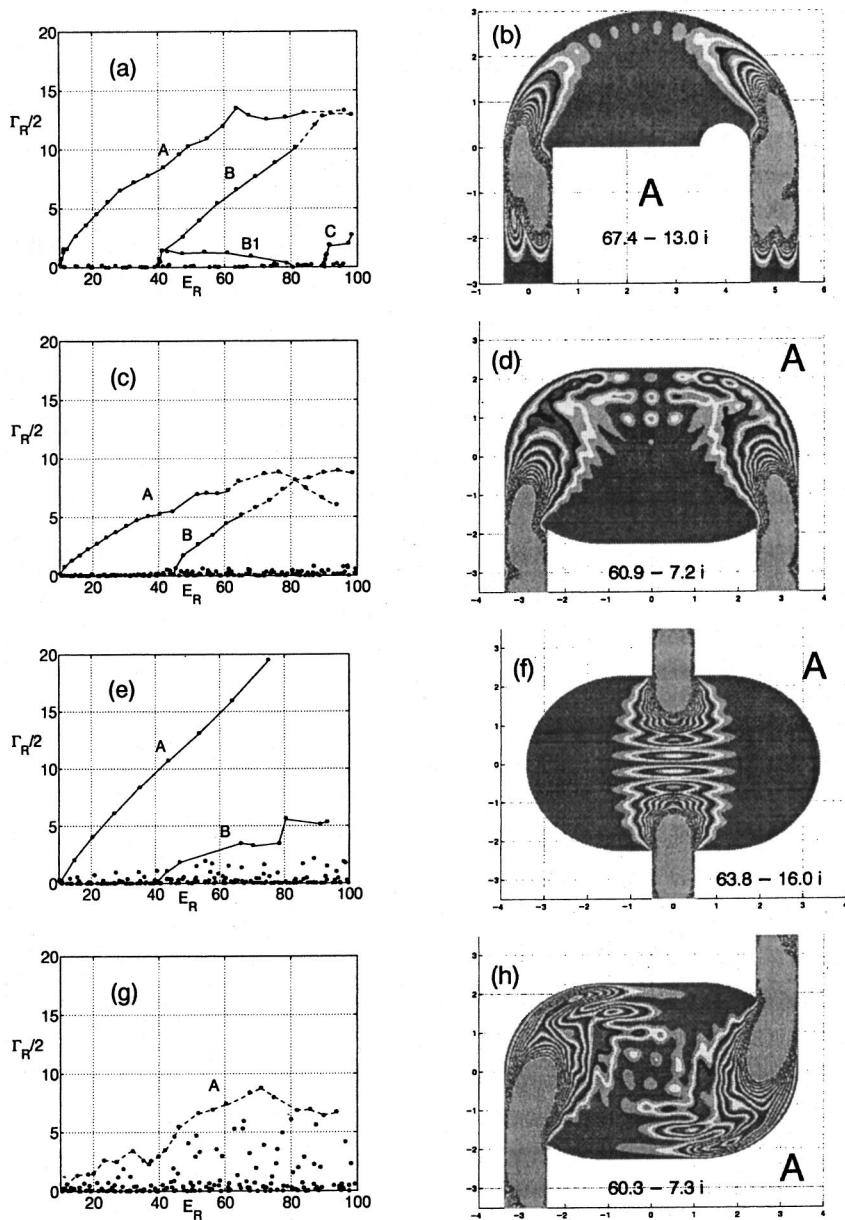


FIG. 1. The poles of the S matrix and a representative picture $|\Phi_R|^2$ of the wave functions of the short-lived states (belonging to the group A) for the SIS (a, b), $B1$ (c, d), $B2$ (e, f) and $B3$ (g, h). The poles of the S matrix (denoted by stars) far from the real axis are connected by lines for guiding the eyes. The energies and widths are in units of the width of the attached waveguide.

analysis and the classical results in spite of the small value of the wave vector k of the propagating waves.

In the SIS and $B1$ with dominant WGM, the largest peak in the $P(L)$ spectrum can be identified with the length of the path of the WGM trajectories calculated classically. In contrast to the SIS, the classical trajectories of the $B1$ with small L are split into two parts: one bounce at the convex boundary and to two bounces, respectively. The number of paths with two bounces is much smaller than that with one bounce in full agreement with the expectation. Typical pictures of these trajectories are shown near the corresponding peaks in the histogram Fig. 2(f). In both cases, SIS and $B1$, smaller peaks can be identified with other trajectories that are, however, of minor importance for the transport. The energy-dependent conductivity G [especially of the SIS, Fig. 2(a)] reflects the strong channel-channel coupling between the two channel modes at $E > 4\pi^2$, which is responsible for the high conductance also at higher energies.

In the $B2$ billiard, two peaks of comparable height appear in the $P(L)$ spectrum [Fig. 2(h)]. A representative wave function of the states belonging to the first peak is displayed in Fig. 1(f) while another one for the second peak is shown in Fig. 3. In the first case, channel-channel coupling creates effectively one channel while there are effectively two channels in the second case. The corresponding lengths L differ by about a factor 2. This is in agreement with the differences of the paths calculated classically for the two highest peaks in Fig. 2(i) without any bouncing and with two bouncings at the convex boundary of the cavity, respectively. The conductivity of the $B2$ billiard [Fig. 2(g)] is determined only partly by channel-channel coupling.

The differences between the BBM case ($B2$) and the two WGM cases (SIS and $B1$) consist in the following.

The $P(L)$ spectrum is dominated by one peak at small L in the WGM cases, while there are two peaks of less height in the BBM case.

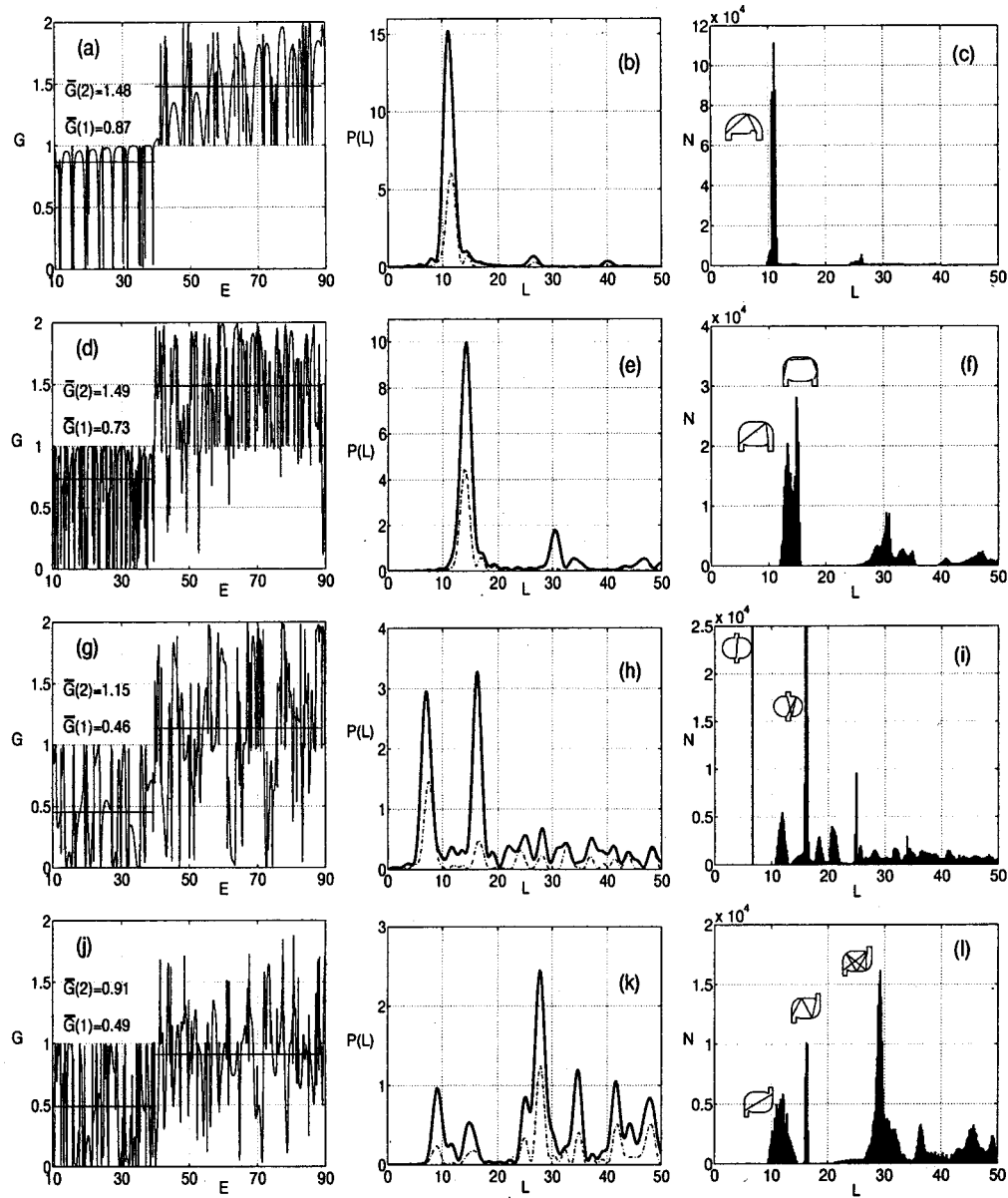


FIG. 2. The conductance $G(E) = \sum_{m,n} |t_{mn}|^2$ (calculated quantum mechanically), the corresponding power spectrum $P(L)$, and the histogram of the (classically calculated) trajectories for conductance as a function of the length L for the SIS (a, b, c), B1 (d, e, f), B2 (g, h, i), and B3 (j, k, l). In (a, d, g, j), $\bar{G}(1)$ and $\bar{G}(2)$ denote the mean value of the conductance in the energy intervals $\pi^2 < E < 4\pi^2$ and $4\pi^2 < E < 9\pi^2$, respectively. In (b, e, h, k), the total power spectrum $P_{tot}(L) = \sum_{m,n} |t_{mn}(L)|^2$ of the transmission amplitudes (thick lines) in the energy interval $\pi^2 < E < 9\pi^2$ and the power spectrum of the transmission amplitudes $|t_{11}(L)|^2$ in the energy region $\pi^2 < E < 4\pi^2$ with two open channels in each lead (dash-dotted lines) are shown. Typical classical trajectories are displayed near the corresponding bins in (c, f, i, l). Note the different scales of $P(L)$ in (b, e, h, k).

The $|t_{11}(L)|^2$ spectra (defined in the energy range $\pi^2 < E < 4\pi^2$) are dominated in all three cases by one peak at small L the height of which is, however, smaller in the BBM case than in the WGM cases.

$\bar{G}(1)$ and $\bar{G}(2)$ are smaller in the BBM case than in the two WGM cases.

The results for the B3 billiard do not show any pronounced peaks in the power spectrum at short lengths L . The mean conductivity is close to the classical value in accordance with the prediction of random matrix theory.²

In Fig. 4, we present the power spectra of the reflection amplitudes for the four billiards studied above. Additionally, we show in each case the wave function of a state lying at the energy where the conductance is minimal. In contrast to the power spectra $P(L)$ of the conductance, the power spectra of the reflection show more pronounced peaks for the B2 and B3 billiards than for the SIS and B1. They appear at comparably large L . In any case, the peaks in the power spectra of the conductance and reflection are at different lengths L for every cavity. This holds especially for the first

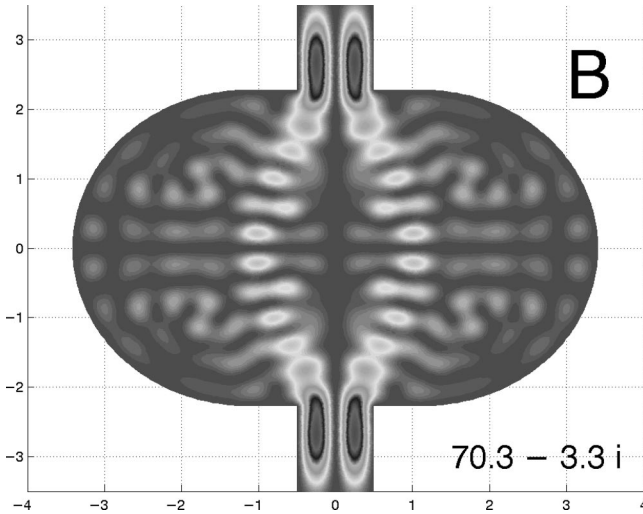


FIG. 3. A representative picture $|\Phi_R|^2$ for the wave functions of the states that belong to the second peak of $P(L)$ at $L \approx 16$ for the $B2$.

peak of the power spectrum for the reflection in the $B2$, which lies between the two BBM peaks of the power spectrum for the transmission.

In Table I, the results obtained for the conductivity from the quantum mechanical calculations are compared with those from the classical calculations. It is remarkable that the conductivity is determined, to a great deal, by trajectories of the WGM type in the classical calculations as well. Their contribution is about 45% and 28% of trajectories for the SIS and the $B1$, respectively. It is smaller in the latter case since the boundary of the $B1$ is not convex everywhere in contrast to that of the SIS. In the quantum mechanical calculations for the SIS and $B1$, the conductivity is maximum at low energy with one open channel. It decreases with increasing energy.

The small conductivity of the $B2$ at low energy (Table I, one channel) is rather unexpected at first sight, since the classical path corresponding to the BBM trajectories is the direct one. Their contribution is, in the classical calculations, however, only about 7% of the total number of the transmitted trajectories, whereas the WGM trajectories contribute about 11%. That means the trajectories occupy, to a large part, the available inner space of the billiard, resulting in a reduction of the conductivity. This tendency can be seen also in the quantum mechanical calculations, see Figs. 1(e) and 3.

Further, we calculated quantum mechanically the $|t_{nm}|^2$ for five open channels in each lead ($n, m = 1, \dots, 5$) in the energy range $(5\pi)^2 < E < (6\pi)^2$ for the $B1$ billiard (Table II), the corresponding Fourier transforms of the $|t_{nm}|^2$ (Fig. 5) and, for illustration, the number of classical trajectories traveling through the billiard (Fig. 6). In the classical calculations, we included only trajectories with lengths smaller than 20 according to the results shown in Fig. 2(f). The angle Φ is determined by the trajectory going into the billiard (Φ_{in}) or leaving it (Φ_{out}). Using the quantum mechanical correspondence between energy and angle $\Phi = \arctan[\pi n / \sqrt{E - (\pi n)^2}]$, we divide the $|\Phi_{in}| - |\Phi_{out}|$ plane into 5×5 blocks corresponding to the transmissions $|t_{nm}|^2$.

The angle Φ is measured with respect to the normal of the attachment line between lead and billiard. The trajectories that enter and leave the cavity at an angle around $\Phi \approx 0$ can be identified with trajectories of the WGM type. The dark straight line can be associated with trajectories that bounce once off the linear boundary of the billiard ($\Phi \approx \pi/4$). Most trajectories with large angles are longer than 20 and do not appear in Fig. 6 since they are not taken into account in the classical calculations.

IV. DISCUSSION OF THE RESULTS

Comparing the results for the different billiards (performed for the ballistic regime), we see the strong influence of the lead orientation onto the resonance wave functions and the conductance or reflection. The results can be understood on the basis of Eq. (5) that involves the coupling coefficients \tilde{W}_R^c between the *resonance* states and the channel wave functions in the leads. It follows as listed below.

The most effective attachment of the leads for a selection of special modes and a high conductance is the symmetrical one with $\tilde{W}_R^c \approx \tilde{W}_R^{c'}$.

The destructive interferences in the transmission amplitudes are reduced when the number of states *and* channels is effectively reduced.

The first condition is fulfilled for the SIS and the $B1$ with selection of the WGM as well as for the $B2$ with selection of the BBM. It is *not* fulfilled for the $B3$ where \tilde{W}_R^c is large for the WGM along the upper boundary but $\tilde{W}_R^{c'}$ is small, and vice versa for the WGM along the lower boundary. Although the number of WGM is more or less the same in the $B3$ as in the $B1$, the conductance is very different in the two cases.

The second condition is fulfilled to the maximum by resonance trapping. The differences in the coupling coefficients \tilde{W}_R^c between the *resonance* states R and the wave functions of the channels c are larger than those in the original coupling coefficients $W_R^{c(d)}$ between the discrete states and the channels. A few of the \tilde{W}_R^c may reach the maximum possible value determined by Eq. (6) while those of the remaining ones approach zero, meaning that they are almost decoupled from the channels. Due to the large coupling coefficients between the special states and the channel wave functions, the channels are coupled via these states. As a consequence, not only the number of states is effectively reduced, *but also* the number of channels is effectively scaled down. In this manner, a few special quantum mechanical states may be selected by the attachment of the leads to the cavity whose number is, in any case, smaller than the total number of states. Further, the special states are coupled mainly to some channels whose number is effectively smaller than (or at most equal to) the total number of open channels (for illustration see Fig. 1 and Ref. 24 for quantum billiards and also²⁶ for nuclei). Thus, the interferences between the transmission amplitudes are reduced by the phenomenon of resonance trapping.

Another illustration for the effective reduction of the number of channels, to which the special states are coupled,

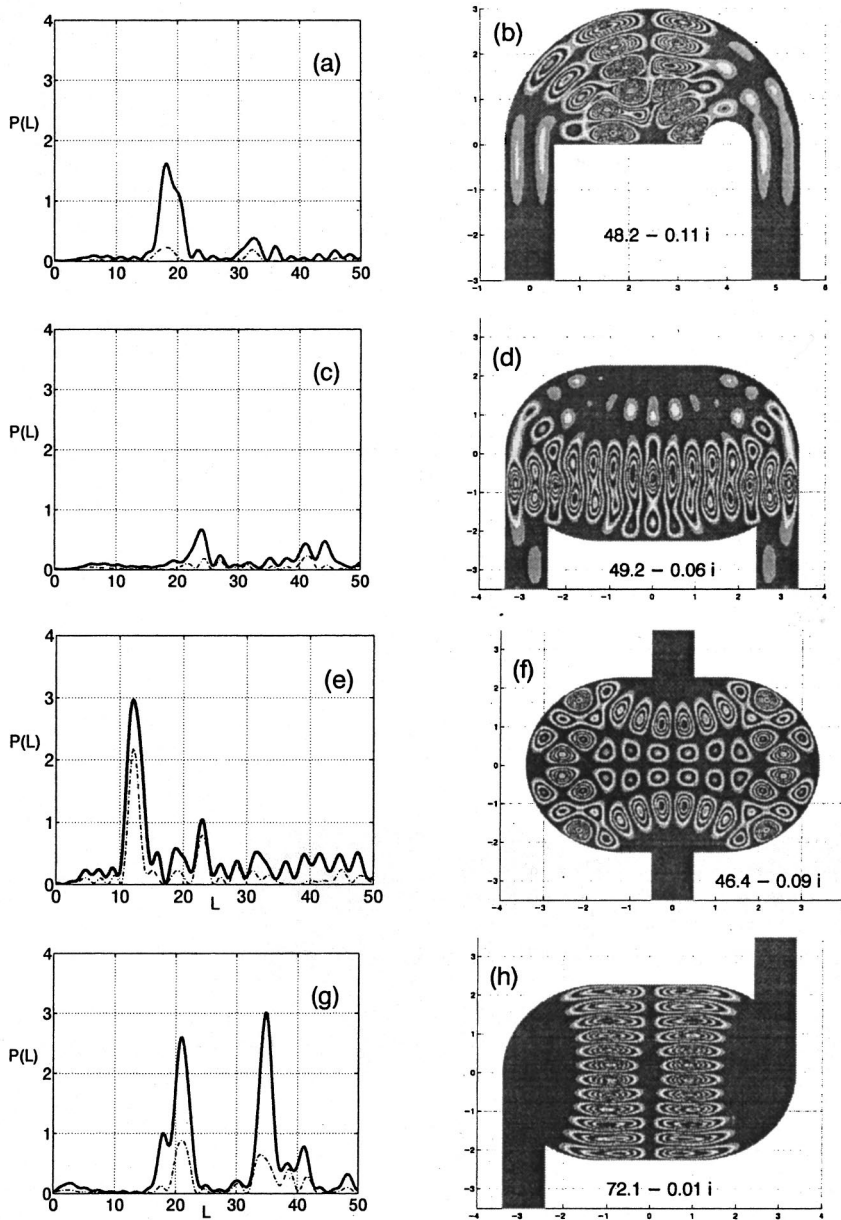


FIG. 4. The power spectrum $P_{tot}(L) = \sum_{m,n} |r_{mn}(L)|^2$ for the reflection amplitudes (thick lines) in the energy region $\pi^2 < E < 9\pi^2$ and $|r_{11}(L)|^2$ in the energy region $\pi^2 < E < 4\pi^2$ with two open channels in each lead (dash-dotted lines) for the SIS (a), B1 (c), B2 (e), and B3 (g). The wave function $|\Phi_R|^2$ of a state, lying at an energy where the conductance is small, for the SIS (b), B1 (d), B2 (f), and B3 (h).

is shown in Fig. 6 where the quantum mechanical transmission matrix elements, calculated with account of five channels (modes) in each lead, are mapped onto the classical transmission matrix, calculated with account of paths shorter than 20. The classical transmission through short paths ($L \leq 20$) corresponds to the quantum mechanical transmission through the special states with at most four (out of five)

TABLE I. The conductance G/Z for different billiards with different number Z of channels.

Billiard type	1 channel	2 channels	3 channels	Classical
SIS	0.87	0.75	0.74	0.66
B1	0.74	0.73	0.65	0.63
B2	0.46	0.56	0.56	0.57
B3	0.49	0.46	0.56	0.53

channels. In the energy region between $25\pi^2$ and $36\pi^2$ there are, in the quantum mechanical calculations with five channels, however, contributions also from other states with longer paths to the transmission (Fig. 5). While the Fourier transforms of $|t_{mn}|^2$ with $mn = 11, 12, 14, 33, 34,$ and 44 have a well-expressed peak around $L \approx 14$ to 15 , this is not so in the other cases. The Fourier transforms with $mn = 22, 23$ are strongly peaked around $L = 30$ while those with $mn = 13, 15, 24, 25, 35,$ and 45 are distributed over different $L > 15$ and that with $mn = 55$ even over $L > 27$. As can be seen from these numbers, the quantum mechanical contributions with $L < 20$ to the conductance are restricted to four channels in each lead, indeed. That is in full accordance to the classical picture. The increasing contributions to the conductance from states with larger L weaken, however, the channel-channel coupling, and the effective number of channels approaches the number Z of independent channels. The

TABLE II. The values $|t_{nm}|^2$ for the $B1$ billiard with $n, m = 1, \dots, 5$.

n	m	$ t_{nm} ^2$
1	1	0.45
1	2	0.10
1	3	0.05
1	4	0.06
1	5	0.10
2	2	0.18
2	3	0.09
2	4	0.17
2	5	0.10
3	3	0.31
3	4	0.14
3	5	0.08
4	4	0.31
4	5	0.07
5	5	0.16

results of classical calculations without the restriction to small L (not shown) correspond to this result of the quantum mechanical studies.

According to the numerical results for $|t_{nm}|^2$ with five channels in each lead (Table II), the contributions to the conductance from the $|t_{mn}|^2$ with a single peak around $L \approx 14$ to 15 are mostly larger than those from the other $|t_{mn}|^2$. Nevertheless, the contributions from states with paths $L > 20$ have to be taken into account. In all the cavities considered by us, the conductance approaches the classical value with increasing number of channels (Table I). For the $B1$ with

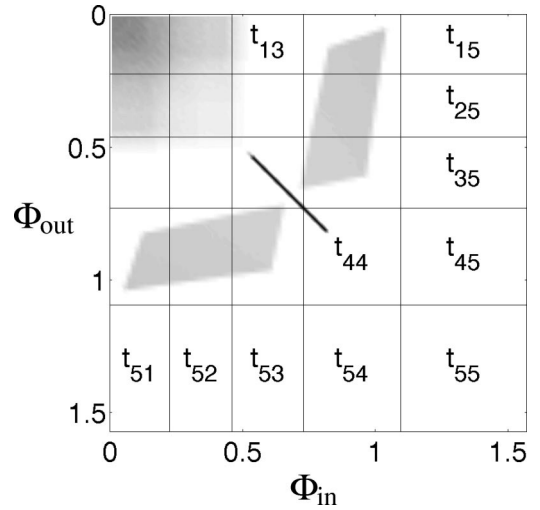


FIG. 6. The transition matrix calculated classically for the $B1$ as a function of the angle of the ingoing and outgoing waves at which the classical trajectories pass the attachment of the leads. The length of the trajectories is restricted to $L \leq 20$. The transmission coefficients t_{nm} ($n, m = 1, \dots, 5$) of the quantum mechanical calculations for five modes in each lead (Table II) can be mapped onto the figure as indicated.

five channels, we obtain $G/Z = 0.66$.

According to Eqs. (6) and (7), the coupling strength between cavity and lead is finite so that the widths of the special states can reach, by resonance trapping, a maximum possible value only. By this, the conductivity is restricted in value also. In some cases (WGM only along the upper boundary as in the SIS), the conductivity is enhanced, indeed, almost up to the maximum possible value whereas this is not so in the other cases. Neither the BBM modes in the

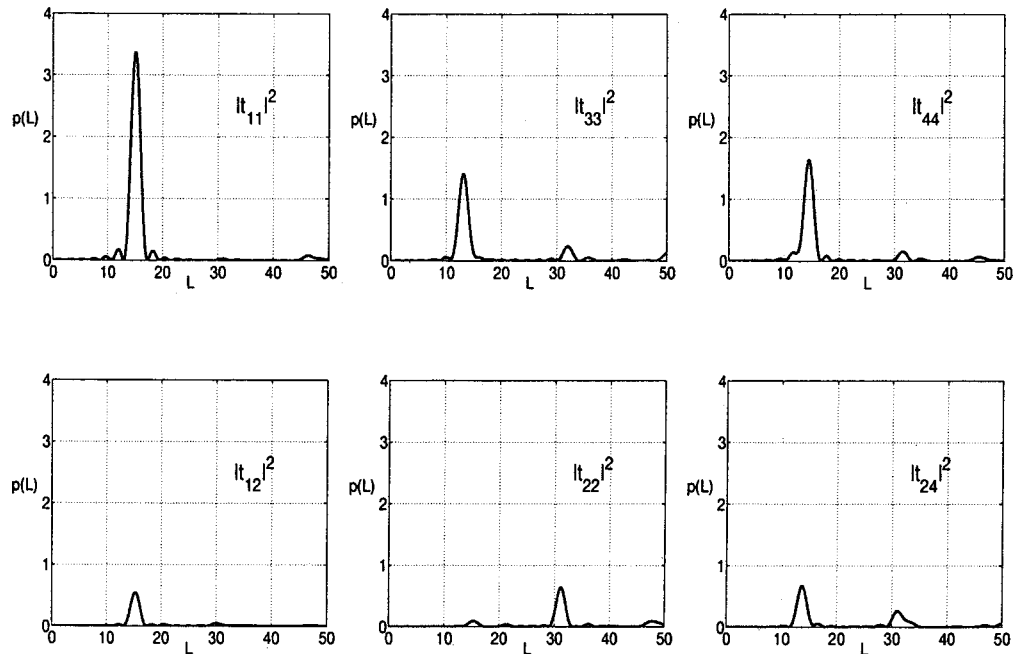


FIG. 5. The power spectra $p(L) \equiv |t_{nm}(L)|^2$ for the $B1$ billiard in the energy region $25\pi^2 < E < 36\pi^2$ with five open channels in each lead. In the figure, only those power spectra are shown for which the height of at least one peak is larger than 0.5.

$B2$ nor the WGM modes in the $B1$ are able to trap completely the remaining states that include special states of the WGM type (along the lower boundary in the $B1$ and along the whole boundary in the $B2$). The maximum value of the conductance can therefore not be reached in these cases. While the special states determine the average properties of observables such as conductance and reflection, the trapped states are responsible for the fluctuations around the mean values. This result is independent of the existence of an internal scatterer inside the cavity. More important than the internal scatterer is the convex lower boundary of the $B1$ in contrast to the linear lower boundary of the SIS.

Characteristic of special states of a certain type is the ratio M^{spec}/M (where M^{spec} is the number of special states and M is the total number of states in a certain energy interval) as well as the dependence of the coupling matrix elements $W_R^{c(d)}$ on the parameter varied. In the cases considered in the present paper, not only the number of WGM is larger than that of BBM, but the WGM overlap stronger and are more stable against small shifts of the leads than the BBM (the last point is studied in Ref. 24 for the SIS). While the WGM are able to trap almost all other states under conditions favorable for them, the BBM do never trap the WGM completely [compare Fig. 1(c) with Fig. 1(e) and see Ref. 24 for the SIS]. These differences are related to the fact that the WGM are more strongly localized than the BBM. While the WGM are localized along the (convex) boundary of the system, the BBM are localized inside the system near the shortest connection between the two leads. Deviations from the shortest distance appear under the influence of the area of the billiard.

In all cases considered by us, the special states (WGM and BBM) accumulate, by resonance trapping, the major part of the coupling strength between system and lead (sum of the widths of *all* states). The close correspondence between the quantum mechanical and classical calculations is related, at least to a great deal, to the existence of these special states. Figure 2 shows the correspondence in relation to the lengths L .

We note that in terms of the semiclassical transmission amplitudes, the spectrum of $t_{mn}(L)$, Eq. (14), is peaked at the lengths L_q of the WGM trajectories connecting the leads due to the rapidly oscillating phase factor in Eq. (16).

Let us now consider the correspondence in relation to the lifetimes (widths). To this aim, we focus on the $B1$ and the $B2$ billiards in the energy interval between the first (π^2) and second ($4\pi^2$) thresholds where the WGM and BBM states are well separated from the other resonance states. In the $B1$ billiard, the special states consist of eleven WGM. The average width of these eleven states is $\bar{\Gamma}_{\text{WGM}} \approx 6.5$. Their contribution to the total coupling strength between system and environment, $\sum_R \bar{\Gamma}_R = 76.6$, is 93%. In the $B2$ billiard, five special states of BBM type accumulate 83% of the total coupling strength. Here, $\bar{\Gamma}_{\text{BBM}} \approx 12.6$ and $\sum_R \bar{\Gamma}_R = 76.1$.

To get an estimation for the mean width $\langle \Gamma \rangle$ of the resonance states in a quantum billiard (*without* taking into account the mixing of the resonance states via the continuum) we use the expression³⁴

$$\rho = M/\Delta E = \frac{A}{4\pi} \frac{2m_{\text{eff}}}{\hbar^2} = \frac{A}{4\pi} \quad (17)$$

for the level density (in units $\hbar^2/2m_{\text{eff}} = 1$, see Sec. II). Here, ΔE is the energy interval considered, M is the number of states, and A is the area of the quantum billiard. The total number of resonance states between the first and second threshold (π^2 and $4\pi^2$) is $M = 3\pi^2 A / (4\pi) \approx 67$ for both billiards, since they have the same area. Also the average coupling strength is approximately the same for the two billiards, see Eqs. (6) and (7). The estimation yields

$$\langle \Gamma \rangle = \sum_R \Gamma_R^d / M \approx \sum_R \bar{\Gamma}_R / M \approx 1.1. \quad (18)$$

It is interesting to compare the quantum mechanical values³⁶

$$\langle \Gamma \rangle = \frac{1}{\tau} \quad \bar{\Gamma}_S = \frac{1}{\tau_S} \quad (19)$$

for the mean lifetimes with those obtained from the classical calculations for the time of flight, where S stands for WGM and BBM, respectively. A rough estimation of the flight time for a particle along the WGM or BBM trajectories gives $\tau^{\text{cl}} = L^{\text{cl}}/v = L^{\text{cl}}/k_n = L^{\text{cl}}/\sqrt{E - n^2\pi^2}$ and therefore

$$\langle \Gamma^{\text{cl}} \rangle = \frac{\sqrt{E - n^2\pi^2}}{L^{\text{cl}}}. \quad (20)$$

We get $\langle \Gamma_{\text{WGM}}^{\text{cl}} \rangle \approx 0.5$ for the WGM trajectories with $L_{\text{WGM}}^{\text{cl}} = 3\pi + 2$ and $\langle \Gamma_{\text{BBM}}^{\text{cl}} \rangle \approx 0.8$ for the BBM trajectories with $L_{\text{BBM}}^{\text{cl}} = 6\pi / (\pi + 1) + 2$ and maximum energy. These values are of the same order of magnitude as the $\langle \Gamma \rangle$ calculated quantum mechanically. The values $\bar{\Gamma}_S$ of the special states, however, are much larger due to resonance trapping. It is $\bar{\Gamma}_{\text{BBM}} / \bar{\Gamma}_{\text{WGM}} \approx \langle \Gamma_{\text{BBM}}^{\text{cl}} \rangle / \langle \Gamma_{\text{WGM}}^{\text{cl}} \rangle = L_{\text{WGM}}^{\text{cl}} / L_{\text{BBM}}^{\text{cl}}$. The relation

$$\bar{\Gamma}_S \propto \frac{1}{L_S^{\text{cl}}} \propto \langle \Gamma_S^{\text{cl}} \rangle \quad (21)$$

holds in all our calculations, see, e.g., Fig. 2(e) in Ref. 24, while $\langle \Gamma \rangle$, Eq. (18), is related to the area of the cavity and is (almost) independent of the manner the leads are attached to it. That means, $\langle \Gamma \rangle$ is *not* related to any special L in contrast to $\bar{\Gamma}_S$. The shortened lifetimes τ_S are an expression for the collective properties of the special states that result from the quantum mechanical phenomenon of resonance trapping. They allow, under certain conditions, an enhancement of the conductance, as discussed above.

All the results obtained in the present study show the close correspondence between the classical and the quantum mechanical characteristics for the transport through billiards of different shape in the strong-coupling regime. This correspondence is achieved by the dynamics of open quantum systems which is determined by the shape of the cavity and the position of the attachment of the leads to it. The dynamics can be understood on the basis of the resonance reaction part (5) of the S matrix that involves the characteristics of the *resonance* states, which are determined not only by the wave

functions of the states of the closed system but also by the influence of the environment onto the properties of the system [including the phenomenon of resonance trapping following from Eqs. (6) and (7)].

V. CONCLUSIONS

For the Bunimovich stadium with two attached leads we have calculated energies, wave functions, and coupling coefficients to the environment (widths). As a result, all these values may change strongly by varying the position of the attached leads. The changes can be seen in observables such as conductance or reflection.

Our study shows that special states exist in open quantum billiards. These states have individual (nongeneric) properties characteristic of the geometry of the system. They have large widths (small lifetimes) due to trapping other states most of which have lost their individual properties they had in the closed cavity, see, e.g., Ref. 22. The wave functions of the special states are localized while those of the trapped states are distributed over the whole cavity. The special states determine, as a rule, the mean properties of observables (such as the conductance) while the trapped states are responsible for the fluctuations around the mean values. The contribution of special states to physically relevant values can be enhanced by the attachment of leads to the billiard in such a manner that the coupling of these states to the channel wave functions is favored. These results are in qualitative agreement with experimental data obtained from quantum dots with different lead alignments.¹⁵ Examples of special states are, above all, the WGM studied in this paper. The BBM are less stable.

The most interesting result of our study is the relation between classical and quantum mechanical properties of the open microwave cavities at low energies. The special states have short lifetimes, corresponding to trajectories with short path length. These states cause the nonrandomness of the system at low energy where the number of channels is small. They are characteristic of the system, and the classical-quantum correspondence does (almost) not depend on the position of the attached leads.

The short-lived special states are localized around the

classical paths with very few bounces at the boundary and are coupled strongly to a small number of effective channels. The lifetimes of these states depend on the geometry of the billiard: they are proportional to the lengths of the classical trajectories. In contrast to this, the long-lived trapped states are delocalized (i.e., distributed over more or less the whole area of the billiard) and coupled very weakly to *all* channels. It should be underlined that the coherent short-lived and incoherent long-lived resonance states exist always together at the same energy. Only the long-lived trapped states can cause the randomness of the system.

We conclude the following. The classical properties of dynamical systems are manifest in quantum mechanical characteristics of open systems even at low energy where the level density and the number of open channels are small. The classical properties are related, above all, to the properties of special states that exist in the closed system and whose special features may be strengthened by coupling the system to an environment by an appropriate position of the leads. This enhancement is caused by the phenomenon of resonance trapping. It is accompanied (i) by the formation of long-lived states in the same energy region which contribute incoherently to the observable values and (ii) by a reduction of the effective number of channels for the decay of the special states. Due to the destructive interferences between the short-lived special states and the long-lived trapped states, an enhancement (reduction) of observable values appears only at low-level density. This result, discussed in the present paper with the example of the transmission (reflection) through quantum billiards, is expected to be true also for other observables and, above all, for real quantum systems such as quantum dots.

ACKNOWLEDGMENTS

We thank D. V. Savin and V.V. Sokolov for useful discussions and H. Schomerus for the critical reading of the manuscript. This work was supported in part by the Russian Foundation for Basic Research Grants Nos. 00-02-17194, 01-02-16077, the Heisenberg-Landau program of the BLTP, JINR, the Czech grant GAAV A1048101, and by the "Foundation for Theoretical Physics" in Slemeno, Czech Republic.

*Email address: rashid@thsun1.jinr.ru

†Email address: knp@tnp.krasn.ru

‡Email address: rotter@mpipks-dresden.mpg.de

§Email address: seba@fzu.cz

¹O. Bohigas, M. J. Giannoni, and C. Schmit, *Phys. Rev. Lett.* **52**, 1 (1984).

²C. W. J. Beenakker, *Rev. Mod. Phys.* **69**, 731 (1997).

³T. Guhr, A. Müller-Groeling, and H. A. Weidenmüller, *Phys. Rep.* **299**, 190 (1998).

⁴Y. Alhassid, *Rev. Mod. Phys.* **72**, 895 (2000).

⁵T. A. Brody, J. Flores, J. B. French, P. A. Mello, A. Pandey, and S. S. M. Wong, *Rev. Mod. Phys.* **53**, 385 (1981).

⁶R. Blümel and U. Smilansky, *Phys. Rev. Lett.* **60**, 477 (1988); **64**, 241 (1990); *Physica D* **36**, 111 (1989).

⁷R. A. Jalabert, H. U. Baranger, and A. D. Stone, *Phys. Rev. Lett.*

65, 2442 (1990); H. U. Baranger, R. A. Jalabert, and A. D. Stone, *ibid.* **70**, 3876 (1993); *Chaos* **3**, 665 (1993).

⁸I. Rotter, *Rep. Prog. Phys.* **54**, 635 (1991).

⁹H. Ishio and J. Burgdörfer, *Phys. Rev. B* **51**, 2013 (1995).

¹⁰C. D. Schwieters, J. A. Alford, and J. B. Delos, *Phys. Rev. B* **54**, 10 652 (1996).

¹¹S. Tarucha, D. G. Austing, T. Honda, R. J. van der Hage, and L. P. Kouwenhoven, *Phys. Rev. Lett.* **77**, 3613 (1996).

¹²D. C. Ralph, C. T. Black, and M. Tinkham, *Physica B* **218**, 258 (1996).

¹³O. Agam, N. S. Wingreen, B. L. Altshuler, D. C. Ralph, and M. Tinkham, *Phys. Rev. Lett.* **78**, 1956 (1997).

¹⁴R. Akis, D. K. Ferry, and J. P. Bird, *Phys. Rev. B* **54**, 17 705 (1996); *Phys. Rev. Lett.* **79**, 123 (1997); J. P. Bird, R. Akis, D. K. Ferry, Y. Aoyagi, and T. Sugano, *J. Phys.: Condens. Matter* **9**, 5935 (1997).

- ¹⁵J. P. Bird, R. Akis, D. K. Ferry, D. Vasileska, J. Cooper, Y. Aoyagi, and T. Sugano, *Phys. Rev. Lett.* **82**, 4691 (1999).
- ¹⁶I. V. Zozoulenko, R. Schuster, K.-F. Berggren, and K. Ensslin, *Phys. Rev. B* **55**, 10 209 (1997); T. Blomquist and I. V. Zozoulenko, *ibid.* **61**, 1724 (2000).
- ¹⁷L. Wirtz, J.-Z. Tang, and J. Burgdörfer, *Phys. Rev. B* **56**, 7589 (1997); **59**, 2956 (1999); S. Rotter, J.-Z. Tang, L. Wirtz, J. Trost, and J. Burgdörfer, *ibid.* **62**, 1950 (2000).
- ¹⁸F. M. Dittes, *Phys. Rep.* **339**, 215 (2000).
- ¹⁹R. E. Prange, R. Narevich, and O. Zaitsev, *Phys. Scr., T* **T90**, 134 (2001).
- ²⁰H. Ishio, A. I. Saichev, A. F. Sadreev, and K. F. Berggren, *Phys. Rev. E* **64**, 056208 (2001).
- ²¹H.-J. Stöckmann, *Quantum Chaos: An Introduction* (Cambridge University Press, Cambridge, 1999).
- ²²E. Persson, K. Pichugin, I. Rotter, and P. Šeba, *Phys. Rev. E* **58**, 8001 (1998); P. Šeba, I. Rotter, M. Müller, E. Persson, and K. Pichugin, *ibid.* **61**, 66 (2000).
- ²³I. Rotter, E. Persson, K. Pichugin, and P. Šeba, *Phys. Rev. E* **62**, 450 (2000).
- ²⁴R. G. Nazmitdinov, K. N. Pichugin, I. Rotter, and P. Šeba, *Phys. Rev. E* **64**, 056214 (2001).
- ²⁵Y. H. Kim, M. Barth, H. J. Stöckmann, and J. Bird (unpublished).
- ²⁶S. Drożdż, J. Okońowicz, M. Płoszajczak, and I. Rotter, *Phys. Rev. C* **62**, 024313 (2000).
- ²⁷E. Persson, I. Rotter, H. J. Stöckmann, and M. Barth, *Phys. Rev. Lett.* **85**, 2478 (2000).
- ²⁸I. Rotter, *Phys. Rev. E* **64**, 036213 (2001).
- ²⁹I. Rotter, *Ann. Phys. (Leipzig)* **38**, 221 (1981).
- ³⁰V. V. Sokolov and V. G. Zelevinsky, *Nucl. Phys. A* **504**, 562 (1989); *Ann. Phys. (N.Y.)* **216**, 323 (1992).
- ³¹C. Mahaux and H. A. Weidenmüller, *Shell-Model Approach to Nuclear Reactions* (North-Holland, Amsterdam, 1969).
- ³²K. Pichugin, H. Schanz, and P. Šeba, *Phys. Rev. E* **64**, 056227 (2001).
- ³³H.-J. Stöckmann, E. Persson, M. Barth, Y.-H. Kim, and I. Rotter (unpublished).
- ³⁴M. C. Gutzwiller *Chaos in Classical and Quantum Mechanics* (Springer, New York, 1990).
- ³⁵T. Ando, *Phys. Rev. B* **44**, 8017 (1991).
- ³⁶The relation (19) is true in atomic units $\hbar = |e| = m = 1$ which may differ from the units $\hbar^2/2m_{\text{eff}} = 1$ used in the present paper. The result discussed by us is, however, not influenced by this difference due to the following fact: $\langle \Gamma \rangle$ is (more or less) the same for the different billiards considered in the present paper, while the corresponding $\langle \Gamma^{\text{cl}} \rangle$ differ by a factor of almost 2.